Thermodynamics of multiferroic spin chains

J. Sirker
Department of Physics and Research Center OPTIMAS, University of Kaiserslautern, D-67663 Kaiserslautern, Germany and Max-Planck-Institute for Solid State Research, Heisenbergstr. 1, 70569 Stuttgart, Germany

(Received 24 September 2009; revised manuscript received 1 December 2009; published 26 January 2010)

The minimal model to describe many spin-chain materials with ferroelectric properties is the Heisenberg model with ferromagnetic nearest-neighbor coupling J_1 and antiferromagnetic next-nearest-neighbor coupling J_2. Here we study the thermodynamics of this model using a density-matrix algorithm applied to transfer matrices. We find that the incommensurate spin-spin correlations—crucial for the ferroelectric properties and the analog of the classical spiral pitch angle—depend not only on the ratio $J_2/|J_1|$ but also strongly on temperature. We study small easy-plane anisotropies which can stabilize a vector chiral order as well as the finite-temperature signatures of multipolar phases, stable at finite magnetic field. Furthermore, we fit the susceptibilities of $LiCuVO_4$, $LiCu_2O_2$, and Li_2ZrCuO_4. Contrary to the literature, we find that for $LiCuVO_4$ the best fit is obtained with $J_2 \sim 90$ K and $J_2/|J_1| \sim 0.5$ and show that these values are consistent with the observed spin incommensurability. Finally, we discuss our findings concerning the incommensurate spin-spin correlations and multipolar orders in relation to future experiments on these compounds.

DOI: 10.1103/PhysRevB.81.014419 PACS number(s): 75.10.Jm, 75.40.Mg, 05.70.−a, 05.10.Cc

I. INTRODUCTION

A number of spin-1/2 chain materials have recently been investigated showing multiferroic behavior, i.e., an intricate interplay of magnetic and electric order.[1–7] A microscopic model for the electric ordering based on a spin-current mechanism has been introduced in Ref. 8 and seems to provide an understanding for most of the experimental findings. Here the electric polarization $\boldsymbol{P}$ is related to noncollinear spin-spin correlations, $\boldsymbol{P} \sim \boldsymbol{e}_{ij} \times (\boldsymbol{S}_i \times \boldsymbol{S}_j)$, where $\boldsymbol{S}_i$ is a spin-1/2 operator at site i and $\boldsymbol{e}_{ij}$ is a vector connecting the chain sites i and j. Later it has been shown based on a Ginzburg-Landau theory[9] and symmetry arguments[10] that this coupling between the polarization and magnetization always exists independent of the crystal symmetry. To obtain a noncollinear spin structure on a lattice without geometrical frustration, a minimal model has to contain additional interactions apart from the nearest-neighbor Heisenberg interaction. One possibility are *frustrating* longer-range interactions. For chain materials consisting of edge-sharing copper-oxygen plaquettes such as $LiCuVO_4$, $LiCu_2O_2$, or $Li_2ZrCuVO_4$ the next-nearest-neighbor interaction is particularly relevant leading to the minimal model,

$$H = \sum_r \{J_1(\boldsymbol{S}_r \boldsymbol{S}_{r+1})_{XXZ} + J_2(\boldsymbol{S}_r \boldsymbol{S}_{r+2})_{XXZ} - hS_r^z\}. \qquad (1)$$

Here $(\boldsymbol{S}_r \boldsymbol{S}_{r+i})_{XXZ} = S_r^x S_{r+i}^x + S_r^y S_{r+i}^y + \Delta S_r^z S_{r+i}^z$ with $\Delta \leq 1$ being an exchange anisotropy. For the edge-sharing chains the nearest-neighbor coupling is ferromagnetic ($J_1 < 0$) while the next-nearest-neighbor coupling is antiferromagnetic ($J_2 > 0$). This is the case we want to study here. The external magnetic field is denoted by h. In the classical isotropic model ($\Delta = 1$) without field the frustration leads to a helical spin arrangement with a pitch angle $\phi = \arccos(1/4\alpha)$ for $\alpha = |J_2/J_1| > 1/4$. As in the classical model, the ground state of the quantum model (1) is ferromagnetic for $\alpha < 1/4$. For $\alpha > 1/4$ the ground state is a singlet whose nature has not fully been clarified yet.[11,12] Based on a renormalization-group treatment starting from two decoupled Heisenberg chains ($J_1 = 0$), it has been predicted that any small $J_1 < 0$ produces a finite but tiny excitation gap.[12] Numerically such a gap could not be resolved so far.

Due to the SU(2) spin-rotational symmetry only a quasi-long-range helical order (algebraically decaying) is possible in the isotropic model (1) without field. Whether the correlation functions are indeed algebraically or instead exponentially decaying with a very large correlation length as suggested in Ref. 12 is a question which we will not address here and which is not important for the following discussions. One can in any case still define a pitch angle ϕ by studying the spin-spin correlation functions which, however, turns out to be substantially modified compared to the classical case due to quantum fluctuations.[13] If the SU(2) symmetry is broken by applying either a magnetic field h or by an anisotropy $\Delta < 1$ then the *vector chirality*,

$$\kappa^{(n)} = (\boldsymbol{S}_r \times \boldsymbol{S}_{r+n})^z = \frac{i}{2}(S_r^+ S_{r+n}^- - S_r^- S_{r+n}^+) \qquad (2)$$

can have a nonzero expectation value because this requires only the breaking of the remaining $\mathbb{Z}_2$ symmetry. The vector chirality as defined in Eq. (2) is directly related to the spin current $j_r = j_r^{(1)} + j_r^{(2)}$ which can be obtained from a continuity equation $\partial_t S^z + \partial_r j = 0$. The equation of motion yields $\partial S_r^z = i[H, S_r^z] = -J_1(\kappa_r^{(1)} - \kappa_{r-1}^{(1)}) - J_2(\kappa_r^{(2)} - \kappa_{r-2}^{(2)})$ which leads to the identification $j = J_1 \kappa^{(1)} + 2J_2 \kappa^{(2)}$.[14]

It has been shown that a magnetic field can also stabilize multipolar phases apart from a phase with chiral order, both in the isotropic as well as in the anisotropic case.[14–20] Such multipolar phases are characterized by short-range transverse spin correlations $\langle S_0^+ S_r^- \rangle$ while correlations functions

$$\langle \underbrace{S_0^+ S_1^+ \ldots}_{n \text{ times}} \underbrace{S_r^- S_{r+1}^- \ldots}_{n \text{ times}} \rangle$$

are algebraically decaying in an n-polar phase.

In this paper we want to investigate how the spin-spin correlations of the J_1-J_2 model (1) are affected not only by quantum but also by thermal fluctuations. At the end we want to relate our numerical results with various experiments on edge-sharing copper-oxygen chains. A very powerful numerical method to study the thermodynamics of one-dimensional quantum chains directly in the *thermodynamic limit* is the density-matrix renormalization group applied to transfer matrices (TMRG). Here the Hilbert space is truncated to a small fixed number of states while the temperature is lowered successively. In the calculations presented here we will typically retain $N=60-200$ states both in the system and the environment block. We will present data for temperatures where the algorithm seems to be converged which is judged by comparing results obtained for different numbers of states N. For a detailed description of the TMRG algorithm the reader is referred to Refs. 21–24. In a previous TMRG study the isotropic J_1-J_2 model was investigated, however, correlation functions were not calculated.[25] In other works the thermodynamics was studied based on the exact diagonalization of small chains.[20,26]

The paper is organized as follows: in Sec. II we start with the simplest model with isotropic exchange and without magnetic field paying special attention to the evolution of the incommensurabilities in the spin-spin correlation function with temperature. In Sec. III we then study the effects of a finite exchange anisotropy concentrating on the experimentally relevant case of a small easy-plane anisotropy. In Sec. IV we investigate signatures of multipolar phases, which are stable for finite magnetic field at finite temperatures. Finally, in Sec. V, we relate our numerical results obtained in Secs. II–IV to data for three experimentally well-studied compounds ($LiCuVO_4$, $LiCu_2O_2$, $Li_2ZrCuVO_4$). In particular, we fit the susceptibilities using model (1) which allows us to extract the parameters J_1 and J_2. We also discuss neutron-scattering experiments which give access to the pitch angle and compare to the results for the spin-spin correlation function obtained in Sec. II. Furthermore, we suggest future experiments regarding the realization and observation of multipolar orders. The last section is devoted to a brief summary and some conclusions.

II. THERMODYNAMICS OF THE J_1-J_2 CHAIN

For the isotropic case, $\Delta=1$, without magnetic field it is known that there is a quantum critical point at $\alpha=1/4$ separating a ferromagnetic phase for $\alpha<1/4$ from a phase with a singlet ground state. A tiny gap for $\alpha>1/4$ has been predicted,[12] however, even if this gap really exists it will only show up at extremely low temperatures. In the temperature range accessible numerically, the susceptibility χ smoothly approaches the result for the nearest-neighbor Heisenberg chain known from Bethe ansatz[27] for $\alpha\to\infty$ as is shown in Fig. 1. At the critical point, $\chi(T)$ shows a power-law divergence.[28–30] A thorough investigation of the critical properties using the TMRG algorithm will be presented elsewhere.[31]

Numerically, we can also obtain the inner energy e and the free energy f (see Ref. 24). This gives us the entropy

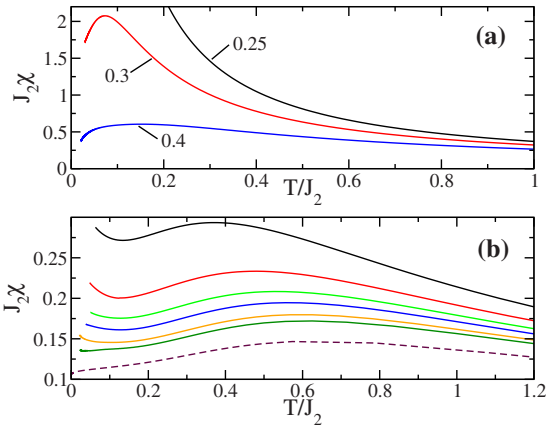

FIG. 1. (Color online) (a) Susceptibilities near the quantum critical point $\alpha=1/4$. (b) Susceptibilities for $\alpha=2.0,1.6,1.2,1.0,0.8,0.6$ (solid lines from bottom to top). For comparison, the result for the nearest-neighbor Heisenberg chain obtained by Bethe ansatz is shown (dashed line).

$s=(e-f)/T$ and the specific heat $C=T\partial s/\partial T$ using a numerical derivative. The results for various α are presented in Fig. 2. For $\alpha=0.4$ we find a sharp low-temperature maximum and a broad maximum at higher temperatures consistent with the calculations of Lu *et al.*, Ref. 25. A similar structure is also found for smaller values of α.[20,25] For $\alpha\geq 0.6$, however, the low-temperature maximum becomes much broader and shifts to higher temperatures so that a second maximum does not appear anymore.

Next, we want to study various correlation functions. At finite temperatures all correlation functions will be exponentially decaying and we can expand any two-point correlation function of an operator O_r as

$$\langle O_0 O_r\rangle - \langle O_0\rangle\langle O_r\rangle = \sum_{j=0}^{\infty} M_j e^{-r/\xi_j}\cos(k_j r). \tag{3}$$

Here M_j is a matrix element, ξ_j is a correlation length, and k_j is the corresponding wave vector. Within the TMRG algorithm both ξ_j and k_j are determined by the ratio of the leading to next-leading eigenvalues of the transfer matrix.[21,24] For large distances $r\gg 1$ the correlation function is domi-

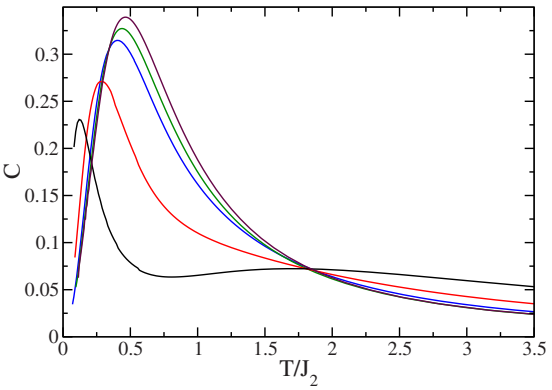

FIG. 2. (Color online) Specific heat for $\alpha=0.4,0.6$, 1.0, 1.4, and 2.0 (from bottom to top).

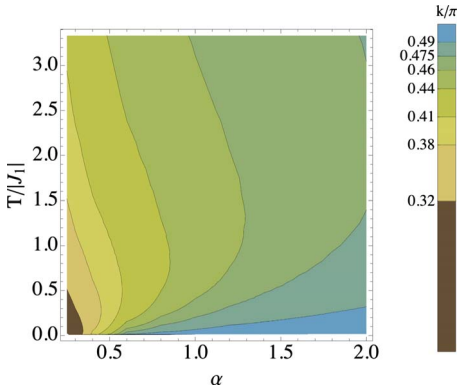

FIG. 3. (Color online) The wave vector k of the spin-spin correlation function depends not only on α but also on temperature.

nated by the largest correlation length and the corresponding wave vector which we will denote as $\xi \equiv \xi_0$ and $k \equiv k_0$ in the following.

Of particular interest is the evolution of the wave vector k for the spin-spin correlation $\langle \boldsymbol{S}_0 \boldsymbol{S}_r \rangle$. This can be seen as the quantum-mechanical analog of the pitch angle of the classical spiral. In Fig. 3 it is shown that k does not only depend on the frustration α but also shows a strong dependence on temperature, in particular, for values of α close to the critical point $\alpha_c = 1/4$. Contrary to the classical case, the pitch angle at low temperatures is very close to $\pi/2$ for $\alpha \gtrsim 0.6$ as is shown in more detail in Fig. 4(a). This means that for these frustration values the spin structure develops an almost perfect (short-range) four-site periodicity at low temperatures. In Fig. 4(b) the extrapolated k value (pitch angle) for zero temperature is shown as a function of α. Our result is in good agreement with an earlier DMRG calculation.[13] Note that k depends nonmonotonically on temperature for $\alpha > \alpha_c$. At intermediate temperatures the pitch angle tends to become more classical [see squares in Fig. 4(b)] meaning that k first decreases with increasing temperature. At high temperatures, on the other hand, the correlations become more commensurate with the lattice and k again approaches $\pi/2$. It is important to stress, however, that the leading correlation length not only becomes very small at high temperatures but that also

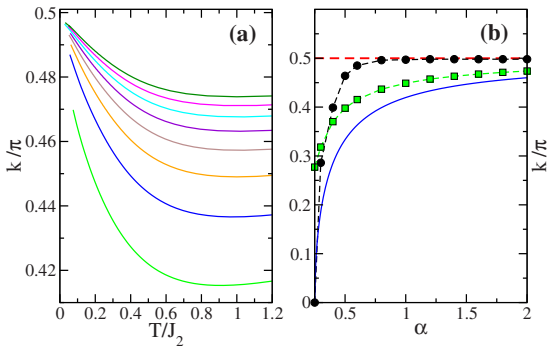

FIG. 4. (Color online) (a) k as a function of temperature for $\alpha = 0.6, 0.8, \ldots, 2.0$ (from bottom to top). (b) Extrapolated k (pitch angle) for zero temperature (circles) and k at $T/J_2 = 1.0$ (squares). The dashed lines are a guide to the eyes. For comparison, the classical pitch angle $\phi = \arccos(1/4\alpha)$ (solid line) is shown.

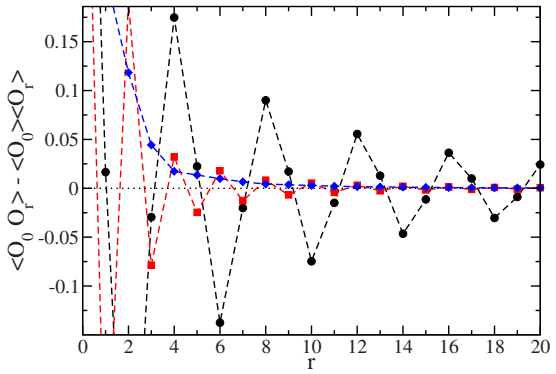

FIG. 5. (Color online) Various correlation functions for $\alpha = 2$ and $T/J_2 = 0.05$. The circles denote the spin-spin ($O_r = \boldsymbol{S}_r$), the squares the dimer ($O_r = \boldsymbol{S}_r \boldsymbol{S}_{r+1}$), and the diamonds the chiral correlation function ($O_r = \boldsymbol{S}_r \times \boldsymbol{S}_{r+1}$). The lines are a guide to the eyes.

other correlation lengths of similar magnitude but with zero wave vector appear in the expansion (3).

One might think that the strong trend toward a formation of a four-site periodic structure with increasing α could be related to a concomitant dimerization. However, as is shown exemplarily in Fig. 5, this is not the case. While substantial dimer and chiral correlations with comparable correlation lengths do exist, both correlation lengths are about a factor two smaller than the spin-spin correlation length.

Another way of defining a quantum analog of the classical pitch angle is the possibility to study at which wave vector q the static spin-structure factor

$$S(q) = \frac{3}{4} + 2\sum_{r=1}^{\infty} \cos(qr)\langle \boldsymbol{S}_0 \boldsymbol{S}_r \rangle \tag{4}$$

is peaked. This definition of the pitch angle is equivalent to the definition in Eq. (3) if the correlation function is dominated by the leading correlation length, i.e., $\xi_0 \gg \xi_j$ for $j \geq 1$. This is the case for all frustration parameters shown in Fig. 6

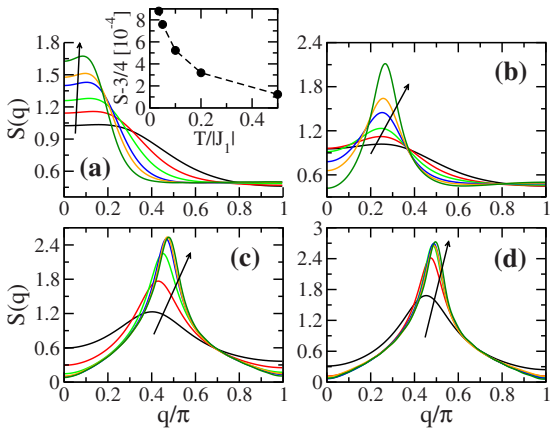

FIG. 6. (Color online) The static spin-structure factor $S(q)$ for temperatures $T/|J_1| = 0.5, 0.2, 0.1, 0.05, 0.035, 0.02$ (along the arrow direction) with (a) $\alpha = 1/4$ (quantum critical point), (b) $\alpha = 0.3$, (c) $\alpha = 0.6$, and (d) $\alpha = 1.0$. The inset of (a) shows the deviation from the sum rule $S \equiv \Sigma_q S(q) = 3/4$.

except for the critical value $\alpha_c=1/4$ [Fig. 6(a)]. Here the structure factor is very flat near $q\sim 0$ meaning that in the expansion (3) comparable correlation lengths exist with a wave vector $k=0$ and with wave vectors which have small incommensurate values. The accuracy of the numerical data can be checked by calculating the sum rule. For all α and all temperatures the sum rule is fulfilled with deviations of the order $10^{-3}-10^{-4}$ as is exemplarily shown in the inset of Fig. 6(a).

III. ANISOTROPIC CASE

In the edge-sharing spin-chain compounds substantial exchange anisotropies exist. For $LiCuVO_4$, for example, the g tensor has been measured by ESR and an exchange anisotropy on the order of 6% has been estimated.[32] This anisotropy is expected to pin the spins to the ab plane and this is indeed observed in experiment.[5,7] Theoretically, one expects that an XXZ-type anisotropy ($\Delta \lesssim 1$) enhances chiral correlations. In this case even long-range chiral order ($\langle \kappa^{(n)} \rangle \neq 0$) is possible at zero temperature in the purely one-dimensional model because only the remaining $\mathbb{Z}_2$ symmetry has to be broken. In previous numerical studies the anisotropic model (1) has already been investigated, the results, however, have been contradictory.[18,33] In Ref. 33 a large region of the phase diagram has been found to be occupied by a dimer phase whereas spin-liquid phases occur for very small and large values of α. In Ref. 18, a dimer phase and spin-liquid phases have again been found but in addition also a chiral phase for $\alpha \gg 1$. Both studies were based on exact diagonalization. In a very recent density-matrix renormalization-group study the anisotropic model at finite magnetization was investigated.[16] A dimer phase was not found to be stable, instead it was shown that for most parameters a chiral phase or a spin-liquid phase (SDW_2 phase) occur.

We will concentrate on one value of anisotropy, $\Delta=0.8$. This is larger than what is expected for the edge-sharing cuprate chains. However, this way the effects of the anisotropy are more obvious and the results should qualitatively be similar to those for realistic values for these materials. To see whether a spin-density wave (SDW), a dimer or a chiral phase is stable we study the longitudinal spin-spin ($O_r=S_r^z$), the dimer-dimer ($O_r=\boldsymbol{S}_r\boldsymbol{S}_{r+1}$), and the chiral-chiral ($O_r=\kappa^{(1)}$) correlation functions. In Fig. 7 results for the corresponding correlation lengths at $\alpha=0.4$ are shown. For correlation functions which decay algebraically at zero temperature we expect that the correlation length diverges as $\xi\sim 1/T$. Studying ξT as in Fig. 7 thus separates long- and short-ranged correlations. In this case we see that the chiral correlation length diverges stronger than $1/T$ indicating that for these parameters we do have long-range chiral order at zero temperature. While the dimer is indeed larger than the chiral correlation length over a wide temperature range, the situation is reversed at low temperatures. Hence a dimer phase can only possibly occur if also interchain couplings are present which might stabilize such an order at intermediate temperatures. That the chiral correlations indeed dominate at low temperatures is shown exemplarily for $T/J_2=0.125$ in Fig. 7(a) where the chiral and longitudinal spin-spin correlation functions are compared. Here the wave vector k of the longitudinal spin-spin correlation function is incommensurate and again shows a strong dependence on temperature [Fig. 7(b)].

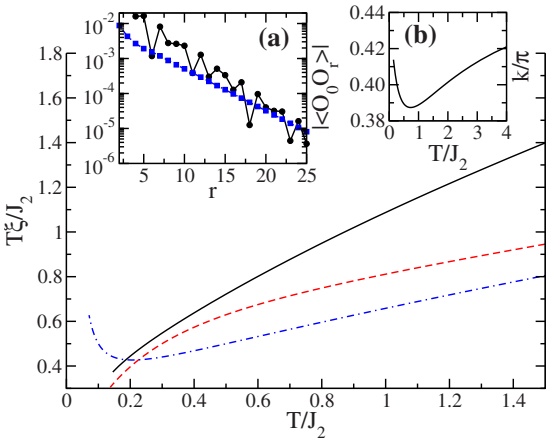

FIG. 7. (Color online) The longitudinal spin (solid line), the dimer (dashed line), and the chiral correlation length (dot-dashed line) for $\alpha=0.4$ and $\Delta=0.8$. At low temperatures the chiral correlation length diverges stronger than $1/T$ indicating long-range order at zero temperature. (a) The longitudinal spin-spin and the chiral correlation functions at $T/J_2=0.125$ showing that chiral correlations dominate. (b) The wave vector k of the longitudinal spin-spin correlation function.

For $\alpha=0.6$, shown in Fig. 8(a), the chiral correlation length is again dominant at the lowest temperatures which are accessible numerically, however, there is no indication for long-range chiral order at zero temperature. Remarkably, all three correlation lengths are of very similar magnitude at low temperatures. This suggest that we are very close or at the phase transition from a phase with long-range chiral order at smaller values of α to a phase which most likely has spin-liquid character with algebraically decaying correlation functions. Indeed, at $\alpha=2.0$ shown in Fig. 8(b) the spin-spin correlation length is clearly dominant with oscillations $k\approx \pi/2$ at low temperatures pointing to an SDW_2 phase. We conclude that if a dimer phase exist at all for $\Delta=0.8$ it has to be confined to a very narrow range of frustration parameters

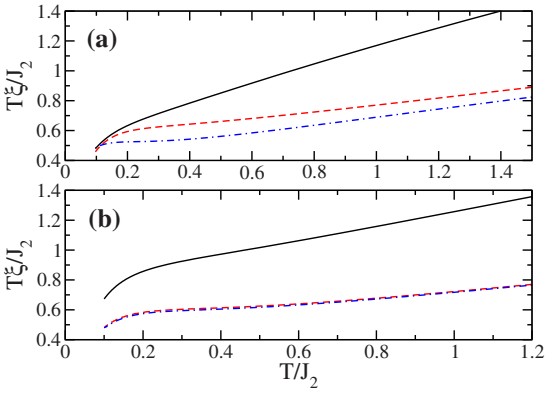

FIG. 8. (Color online) The longitudinal spin (solid line), the dimer (dashed line), and the chiral (dot-dashed line) correlation lengths for $\Delta=0.8$ with (a) $\alpha=0.6$ and (b) $\alpha=2.0$.

$0.4<\alpha<0.6$. In Ref. 33 an unidentified phase was found for $0.3\lesssim\alpha\lesssim0.45$ with symmetries as expected for the chiral phase. For $\alpha\gtrsim0.7$, on the other hand, a spin-liquid phase was predicted with a dimer phase in between these two phases. In our TMRG calculations we never find dominant dimer correlations at low temperatures and our results suggest that a dimer phase might not be stable at all but instead a direct phase transition from the chiral to a SDW_2 phase at $\alpha\approx0.6$ occurs.

IV. FINITE MAGNETIC FIELD: MULTIPOLAR PHASES

In the multiferroic spin-chain compounds a magnetic field can be used to switch the electric polarization. A sufficiently strong field induces a flop of the spins from the easy-plane spiral to a spiral perpendicular to the applied magnetic field. According to the spin-current mechanism this also leads to a rotation of the electric polarization. Such a switching of the ferroelectric polarization by an applied magnetic field has been observed in $LiCuVO_4$ (Ref. 7) as well as in $LiCu_2O_2$.[2] Numerical studies of the J_1-J_2 model have shown that small magnetic fields stabilize the chiral order while multipolar phases become stable at intermediate field strengths before the system ultimately becomes fully polarized for large fields.[14,17–20]

As already eluded to in Sec. I, an algebraic decay of the

$$\langle \underbrace{S_0^+ S_1^+ \ldots}_{n \text{ times}} \underbrace{S_r^- S_{r+1}^- \ldots}_{n \text{ times}} \rangle$$

correlation function is expected in an n-polar ($n\geq2$) phase while the transverse spin-correlation function is gapped. For the oscillations of the longitudinal spin-correlation function we expect, in general,[14,34,35]

$$k_{T\to0}=\frac{\pi}{n}(1-2m), \tag{5}$$

where m is the magnetization. This relation is a direct consequence of the shift of the Fermi points by an applied magnetic field which acts as a chemical potential. For zero field, $n=2$ would correspond to the four-site periodic spin structure discussed previously.

An particular interesting case is $\alpha=0.4$ with $h=0.25J_2$ shown in Fig. 9. Here we find that the longitudinal spin-correlation length is largest at high temperatures, then there is a temperature range where the chiral correlation length dominates while at the lowest accessible temperatures the spin-correlation again dominates and seems to diverge like $1/T$. For zero temperature this field corresponds to a magnetization $m\approx0.15\approx0.3m_{sat}$, [Fig. 9(b)] where $m_{sat}=0.5$ is the saturation magnetization. Comparing with the zero-temperature phase diagrams obtained in Refs. 14 and 17 we see that for these values we are in the SDW_2 phase but very close to the phase boundary with the chiral phase. Our results basically seem to confirm this picture although the oscillations k apparently slightly deviate from the value expected for a $n=2$ multipolar phase even at the lowest temperatures [see Fig. 9(a)]. Our data also show that in a certain temperature window chiral correlations can still be dominant. This might be relevant once interchain couplings are taken into account and might lead to a chiral phase stable at intermediate temperatures while the spins are collinear at higher and lower temperatures. Two magnetic phase transitions have indeed been observed in $LiCu_2O_2$ where first a sinusoidal magnetic order is established followed by a helical order at lower temperatures.[2,36] While the magnetic structure even in the low-temperature phase apparently is much more complicated than a simple planar spiral[36] and the J_1-J_2 model does not seem to capture the essential physics of this compound (see next section) it is nevertheless interesting that even in this very simple model phases might be stable only in a certain temperature range thus possibly giving rise to multiple magnetic phase transitions once interchain couplings are taken into account.

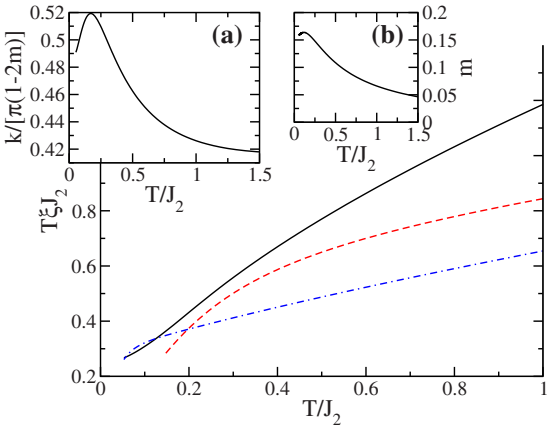

FIG. 9. (Color online) The longitudinal spin (solid line), the dimer (dashed line), and the chiral (dot-dashed line) correlation lengths for $\alpha=0.4$ with $\Delta=1$ and $h=0.25J_2$. (a) The wave vector k of the spin-spin correlation. (b) The magnetization m as a function of temperature.

In Fig. 10 the longitudinal spin-structure factor $S^{zz}(q)$ is shown for $\alpha=0.32$ and $h=0.02J_1$. At low temperatures $S^{zz}(q)$ is peaked at $q=\pi(1-2m)/3$ (dashed line in Fig. 10) indicating an $n=3$ multipolar phase. Thus experimentally a multipolar phase can already be identified at finite temperatures by

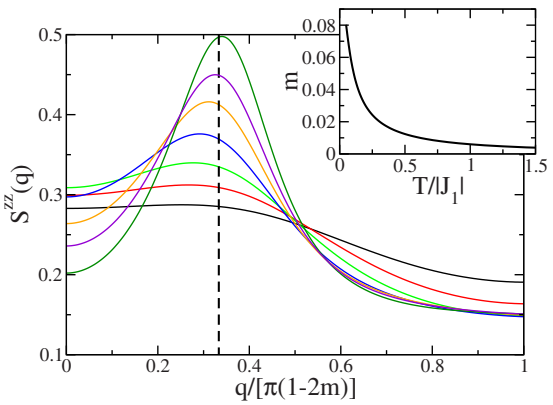

FIG. 10. (Color online) $S^{zz}(q)$ for $\alpha=0.32$, $h=0.02J_1$ and temperatures $T/|J_1|=2.0,1.0,0.5,0.2,0.1,0.07,0.05$ (from bottom to top). The dashed line marks $q/[\pi(1-2m)]=1/3$. The inset shows the magnetization m as a function of temperature.

studying the evolution of the structure factor as obtained in neutron scattering. Such an experiment would be most interesting for a compound close to the quantum critical point $\alpha_c=1/4$ where small magnetic fields are sufficient to stabilize $n=3$ or even $n=4$ multipolar phases.[14,17,20,35] As discussed in detail in Ref. 4 and in the following section, Li_2ZrCuO_4 seems to be a very promising candidate for such a material.

V. MULTIFERROIC SPIN-CHAIN MATERIALS

While in the corner-sharing copper-oxygen chain compounds such as Sr_2CuO_3 and $SrCuO_2$ the antiferromagnetic exchange interaction is of very similar magnitude, $J\sim 2000$ K, a wide range of exchange parameters J_1 and J_2 has been reported in the literature for the edge-sharing compounds. For $LiCuVO_4$, for example, fits of the susceptibility and of neutron-scattering data have led to the estimate $J_1\sim -20$ K and $J_2\sim 50$ K so that $\alpha\sim 2.5$.[5] For Li_2ZrCuO_4, on the other hand, susceptibility and specific-heat data have been fitted by using $J_1\sim -300$ K and $\alpha\sim 0.3$.[4] Given that the chains in these compounds consist of the same edge-sharing copper-oxygen plaquettes, this huge variation in the magnitude of the exchange couplings is surprising.

Here we want to reanalyze the data of three of the best studied multiferroic chain compounds, namely, Li_2ZrCuO_4, $LiCuVO_4$, and Li_2CuO_2. We will concentrate on fitting susceptibility data using

$$\chi_{\mathrm{exp}}=\chi_0+\chi_{J_1\text{-}J_2}. \tag{6}$$

Here χ_{exp} is the experimentally measured susceptibility, χ_0 is a constant contribution due to core diamagnetism and Van-Vleck paramagnetism, and $\chi_{J_1\text{-}J_2}$ is the numerically calculated susceptibility for the J_1-J_2 model (1). Such fits work extremely well for the corner-sharing compounds because the intrachain coupling is about three orders of magnitude smaller than the interchain coupling.[37–41] For $LiCuVO_4$ it has been reported that a three-dimensional (3D) magnetic order becomes established below $T_{3D}\sim 2.3$ K.[6] While this points to intrachain couplings which are only one or at most two orders of magnitude smaller than the interchain couplings, a purely one-dimensional model is still expected to be a good approximation as long as $T\gg T_{3D}$. In Li_2ZrCuO_4 the situation has not fully been clarified yet. A possible phase transition might occur at $T\sim 6$ K.[4] Even if this is a 3D ordering transition, a one-dimensional model should again be valid over a wide temperature range. Therefore the expectation is that the physics of $LiCuVO_4$ and Li_2ZrCuO_4 can largely be understood within the framework of the J_1-J_2 model with the spin-current mechanism being responsible for the multiferroic properties.

The situation for $LiCu_2O_2$, on the other hand, seems to be much more involved.[1–3,36,42] Despite a number of studies, the magnetic structure remains controversial. For instance, both a spiral spin order in the *ab* as well as in the *bc* plane have been reported.[1,3] If the spin-current model is the correct explanation for the observed polarization along the *c* axis[2] then the *bc* spiral must be realized. The two magnetic ordering transitions at comparatively large temperatures, $T\approx 22$ K and $T\approx 24$ K,[36] point to much larger interchain couplings than for the two other compounds discussed above. In fact, it has been found that there are substantial spin correlations not only along the chain direction (*b* axis) but also in the plane of the copper-oxygen plaquettes perpendicular to the chain direction (*a* axis) making the compound at low temperatures almost two dimensional.[42] One might speculate that the reason why the magnetic properties of this material are so different is related to the fact that two different copper sites exist—the in-chain Cu^{2+} and the Cu^{1+} interconnecting different chains. This might lead to substantial charge fluctuations and thus to enhanced magnetic interchain couplings. Nevertheless, a fit of the susceptibility at high temperatures using the J_1-J_2 model might still be useful to obtain an estimate for the magnitude of the J_1 and J_2 couplings.

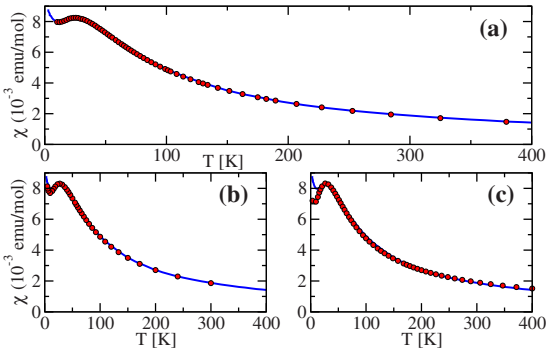

FIG. 11. (Color online) The experimentally measured susceptibility of $LiCuVO_4$ for $H\|c$ (solid line) compared to fits (dots) following Eq. (6) with a gyromagnetic ratio $g=2.313$ (Refs. 6 and 32). (a) The best fit is obtained with $\chi_0=6\times 10^{-5}$ emu/mol, $J_2=91$ K, and $\alpha=0.5$. (b) An alternative fit with $\chi_0=1.4\times 10^{-4}$ emu/mol, $J_2=72$ K, and $\alpha=0.6$. (c) An exchange coupling $J_2=52$ K similar to the one in Ref. 5 can be used with $\chi_0=2.7\times 10^{-4}$ emu/mol, however, the frustration parameter $\alpha=1.0$ chosen to obtain the best fit is still much smaller than the one in Ref. 5 and the fit is much worse than the ones shown in (a) and (b).

The absolute values of the measured maxima of χ already allow some general statements about the magnitude of the exchange constants and the frustration parameters α. In $LiCuVO_4$ and in $LiCu_2O_2$ the susceptibility is about two orders of magnitude larger than in the corner-sharing chain compounds Sr_2CuO_3 and $SrCuO_2$ so that the antiferromagnetic exchange constant J_2 should also roughly be two orders of magnitude smaller. In Li_2ZrCuO_4 the maximum is almost an order larger than in the other two compounds clearly indicating that this compound should be closer to the quantum critical point $\alpha_c=1/4$ than the other two compounds. If the magnetic exchange constants are of comparable magnitude, then α is expected to be largest for $LiCu_2O_2$ and smallest for Li_2ZrCuO_4 with $LiCuVO_4$ having an intermediate frustration parameter.

The susceptibility of $LiCuVO_4$ shown in Fig. 11 has a maximum and a local minimum at low temperatures. If χ can indeed be described by the J_1-J_2 model then a comparison with Fig. 1 indicates that $\alpha\sim 0.5$. The large α used in Ref. 5 can certainly not explain this structure. By performing a fit according to Eq. (6) we find that $J_2=91$ K and $\alpha=0.5$ yields the best fit as shown in Fig. 11(a). A good fit is also possible

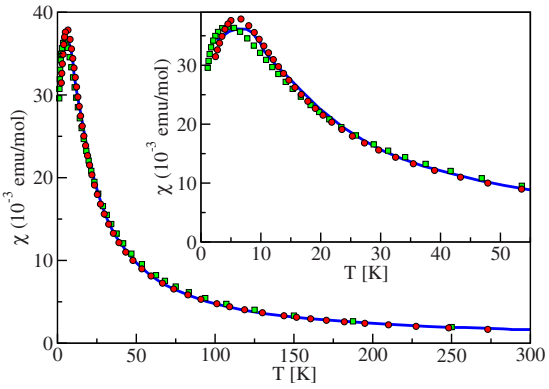

FIG. 12. (Color online) The measured susceptibility (solid line) for Li_2ZrCuO_4 taken from Ref. 4 compared to fits using the J_1-J_2 model. An excellent fit (circles) is obtained using $\alpha=0.3$, $g=2$, and $J_1=-273$ K ($J_2=81.9$ K) with $\chi_0=0$ confirming the analysis in Ref. 4 based on exact diagonalization data. A reasonable fit (squares) is also possible with $\alpha=0.4$, $g=2.2$, $\chi_0=0$, and $J_1=-75$ K. Inset: Blow up of the low-temperature region.

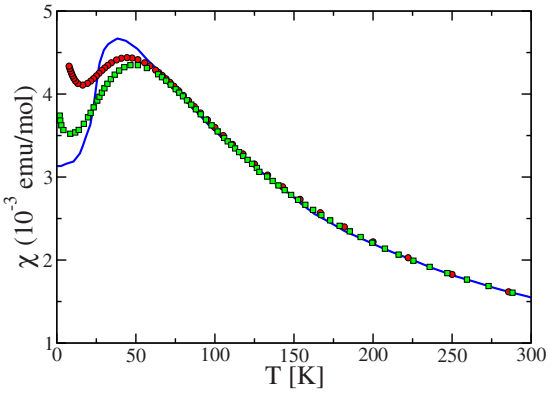

FIG. 13. (Color online) The measured susceptibility (solid line) for $LiCu_2O_2$ with $H\|c$ taken from Ref. 1 compared to fits using the J_1-J_2 model. With $g=2.2$ the best fit is obtained with $\alpha=0.6$, $J_2=120$ K, and $\chi_0=0$ (circles) while for $g=2.3$ a fit with $\alpha=1.6$, $J_2=83$ K, and $\chi_0=0$ works best (squares).

with $J_2=72$ K and $\alpha=0.6$ [Fig. 11(b)]. If we reduce the next-nearest-neighbor exchange to $J_2\sim 50$ K as assumed in Ref. 5 we have to choose $\alpha\sim 1$ to obtain the best-fit possible with this value of J_2 [Fig. 11(c)]. However, such a fit fails to reproduce the low-temperature structure.

The susceptibility data for Li_2ZrCuO_4 have already been analyzed in Ref. 4 by comparing with exact diagonalization data for small rings consisting of up to $N=20$ sites. Finite-size effects are expected to be negligible if $T\gg v/N$, where v is the spin velocity. The spin velocity is on the order of the exchange constant so that the finite-size data for χ should be reliable for $T\gtrsim 20$ K. Given that the maximum of χ is located at $T\approx 7.6$ K, i.e., at temperatures where finite-size effects might play a role, it is helpful to reanalyze the experimental data using the TMRG algorithm which yields results directly for the infinite system. As shown in Fig. 12 very similar fits to the one in Ref. 4 are obtained. While the magnitude of the frustration parameter can only be varied slightly if one wants to obtain a reasonable fit, the exchange parameters change dramatically, for example, from $J_1=-273$ K for $\alpha=0.3$ to $J_1=-75$ K for $\alpha=0.4$. In local-density approximation calculations $J_1=-151\pm 35$ K and $J_2=35\pm 12$ K was found which also will allow for a reasonable fit with a frustration parameter $\alpha\in[0.3,0.4]$.[4] We therefore confirm the main conclusion of Ref. 4 that Li_2ZrCuO_4 is close to the critical point $\alpha_c=1/4$.

Finally, we want to analyze the susceptibility data for $LiCu_2O_2$. As already mentioned, we do not expect that the J_1-J_2 model will describe the susceptibility of this compound at low temperatures and indeed we find that it is impossible to obtain a good fit down to low temperatures (see Fig. 13). If we concentrate on temperatures large compared to the magnetic ordering transitions at $T\sim 20$ K, then a fit is possible and we find that $J_2\approx 80-120$ K. Because the susceptibility can only be fitted at high temperatures, the frustration parameter cannot be fixed precisely.

It is, however, important to note that the best fits for all three compounds yield values of $J_2\lesssim 100$ K while $J_1\sim -200$ K. This confirms our expectation that these materials consisting of the same edge-sharing copper-oxygen plaquettes should have very similar magnetic exchange constants as is also the case for the corner-sharing chain compounds. The values we obtain from the susceptibility fits are consistent with values in the literature for $LiCu_2O_2$ ($J_1\sim -120$ K, $J_2\sim 80$ K) (Refs. 1 and 2) and for Li_2ZrCuO_4.[4] For $LiCuVO_4$, however, we find values which differ dramatically from the values given in Ref. 5 which later were also used in a number of other publications. We want to stress again that these values are not consistent with the latest susceptibility data.[6] An analysis of neutron-scattering data using a standard spin-wave dispersion which seems to confirm these values[5] is in our opinion not applicable here. In such an analysis the magnon bandwidth is directly determined by the bare exchange couplings while the stark deviation of the quantum from the classical pitch angle [see Fig. 4(b)] suggests that the frustration parameter is strongly renormalized due to quantum fluctuations.

The pitch angle measured experimentally in Ref. 5 of $\phi\approx 83.7°$ is in fact in excellent agreement with the frustration parameters $\alpha=0.5-0.6$ obtained from the fits in Fig. 11. According to Fig. 4(b) we have a quantum pitch angle $\phi\approx 83.5°$ for $\alpha=0.5$ and $\phi\approx 87.3°$ for $\alpha=0.6$. It is important to stress again that only in the classical model large frustration parameters are needed to obtain pitch angles close to 90°. We expect, according to Fig. 4(a), that the pitch angle in $LiCuVO_4$ can be reduced by 15–20 % by increasing the temperature to $T\sim J_2\sim 90$ K. For Li_2ZrCuO_4 the magnetic structure has not been studied so far. The pitch angle for $\alpha=0.3$ at zero temperature obtained from our numerical calculations is $\phi\approx 51.5°$. Here we expect a large variation with temperature [see Figs. 3 and 6(b)] and it would be interesting to see if this can also be observed experimentally. For $LiCu_2O_2$ a pitch angle $\phi\approx 62.6°$ has been measured.[1,2] Such a small pitch angle cannot be explained within the J_1-J_2 model given that $\alpha\gtrsim 0.6$ according to the fits shown in Fig. 13. We are therefore again lead to the conclusion that the J_1-J_2 model cannot explain the experimental data for this compound.

VI. CONCLUSIONS

The rich physics of the J_1-J_2 model with ferromagnetic nearest-neighbor coupling J_1 and antiferromagnetic next-nearest-neighbor coupling J_2 has attracted a lot of interest recently. The phase diagram for this model including exchange anisotropies and magnetic fields has been addressed in a number of numerical studies.[13,14,16–20] Here we have shown that the physical properties of this simple model are even more intriguing if the interplay of quantum and thermal fluctuations is taken into account. In particular, we found that the incommensurate oscillations of the spin-spin correlation function (the quantum analog of the pitch angle of the classical spiral order) do not only strongly depend on the frustration parameter $\alpha=J_2/|J_1|$ but also on temperature. For zero temperature we find an incommensurability (pitch angle) ϕ for $\alpha \gtrsim 0.6$ which is very close to 90° in the quantum model and thus very different from the classical pitch angle $\phi=\arccos(1/4\alpha)$ in agreement with an earlier study.[13] At temperatures $T \sim J_2$, however, the pitch angle is much closer to the classical value for $\alpha \gtrsim 0.5$. Furthermore, we find a very strong temperature dependence of the pitch angle for frustration parameters close to the critical point $\alpha_c=1/4$. We therefore expect that the wave vector where the static spin-structure factor for Li_2ZrCuO_4 is peaked—a compound which according to Ref. 4 and the susceptibility analysis performed here has a frustration parameter $\alpha \sim 0.3-0.4$—varies significantly with temperature. For this range of frustration parameters we find that a small easy-plane anisotropy (at zero magnetic field) leads to long-range chiral order even in the purely one-dimensional model.[43] We could, however, find no evidence for the dimer phase which was predicted in Ref. 33 for the anisotropic case for larger frustration parameters. Another observation which again might be relevant for future studies on Li_2ZrCuO_4 is that small magnetic fields (which would correspond to 5–7 T for Li_2ZrCuO_4) can stabilize an SDW_3 ($n=3$ multipolar) phase for $\alpha \sim 0.3$. We suggest that such a phase can already be identified by neutron scattering at finite temperatures by monitoring at the same time the peak position $q_{\max}$ of the static longitudinal structure factor and the magnetization m. The signature of the SDW_3 phase would be that $q_{\max} \rightarrow \pi(1-2m)/3$ for $T \rightarrow 0$.

We also reanalyzed the susceptibility data for $LiCuVO_4$. Here the newer data in Ref. 6 seem to be of much better quality than the older data in Ref. 5. The newer data clearly show that the exchange parameters $J_1 \sim -20$ K, $J_2 \sim 50$ K, and $\alpha=2.5$ used in Ref. 5 do not yield a reasonable fit. These exchange parameters also seem very unlikely given that they deviate significantly from those in other edge-sharing copper-oxygen chains. Our analysis shows that the susceptibility data are best fitted with $J_2 \approx 70-90$ K and $\alpha=0.5-0.6$.

In $LiCu_2O_2$ two magnetic ordering transitions already occur at temperatures $T_{3D} \sim 20$ K and an analysis based on the purely one-dimensional J_1-J_2 model clearly cannot be as successful as for $LiCuVO_4$ and Li_2ZrCuO_4. For $T \gg T_{3D}$ we have shown that a reasonable fit of the susceptibility is nevertheless possible leading to $J_2 \sim 80-120$ K. The frustration parameter remains, however, ambiguous in such a high-temperature fit and we find $\alpha \in [0.6, 1.6]$ with the best fit being obtained for $\alpha=0.6$.

Based on the best fits of the susceptibilities we conclude that all three considered compounds seem to have very similar exchange constants $J_1 \sim -200$ K and $J_2 \lesssim 100$ K. The frustration parameter, on the other hand, varies from $\alpha \approx 0.3$ for Li_2ZrCuO_4, $\alpha=0.5-0.6$ for $LiCuVO_4$ to $\alpha \gtrsim 0.6$ for $LiCu_2O_2$. The parameters found here for $LiCuVO_4$ are fully consistent with the measured pitch angle ~84°. For $LiCu_2O_2$, on the other hand, the small measured pitch angle ~63° cannot be explained within the J_1-J_2 model stressing again that this model is not sufficient to explain the experimental data for this compound. The smallest pitch angle is expected for Li_2ZrCuO_4. Based on our numerical calculations we predict $\phi \sim 53°$.

ACKNOWLEDGMENTS

J.S. thanks I. McCulloch, S. Drechsler, A. Furusaki, P. Horsch, and J. Richter for valuable discussions.

[1] T. Masuda, A. Zheludev, A. Bush, M. Markina, and A. Vasiliev, Phys. Rev. Lett. **92**, 177201 (2004).
[2] S. Park, Y. J. Choi, C. L. Zhang, and S.-W. Cheong, Phys. Rev. Lett. **98**, 057601 (2007).
[3] S. Seki, Y. Yamasaki, M. Soda, M. Matsuura, K. Hirota, and Y. Tokura, Phys. Rev. Lett. **100**, 127201 (2008).
[4] S.-L. Drechsler, O. Volkova, A. N. Vasiliev, N. Tristan, J. Richter, M. Schmitt, H. Rosner, J. Málek, R. Klingeler, A. A. Zvyagin, and B. Büchner, Phys. Rev. Lett. **98**, 077202 (2007).
[5] M. Enderle, C. Mukherjee, B. Fak, R. K. Kremer, J.-M. Broto, H. Rosner, S.-L. Drechsler, J. Richter, J. Malek, A. Prokofiev, W. Assmus, S. Pujol, J.-L. Raggazzoni, H. Rakoto, M. Rheinstädter, and H. M. Rønnow, Europhys. Lett. **70**, 237 (2005).
[6] N. Büttgen, H.-A. Krug von Nidda, L. E. Svistov, L. A. Prozorova, A. Prokofiev, and W. Aßmus, Phys. Rev. B **76**, 014440 (2007).
[7] F. Schrettle, S. Krohns, P. Lunkenheimer, J. Hemberger, N. Büttgen, H.-A. Krug von Nidda, A. V. Prokofiev, and A. Loidl, Phys. Rev. B **77**, 144101 (2008).
[8] H. Katsura, N. Nagaosa, and A. V. Balatsky, Phys. Rev. Lett. **95**, 057205 (2005).
[9] M. Mostovoy, Phys. Rev. Lett. **96**, 067601 (2006).
[10] T. A. Kaplan and S. D. Mahanti, arXiv:0808.0336 (unpublished).
[11] S. R. White and I. Affleck, Phys. Rev. B **54**, 9862 (1996).
[12] C. Itoi and S. Qin, Phys. Rev. B **63**, 224423 (2001).
[13] R. Bursill, G. A. Gehring, D. J. J. Farnell, J. B. Parkinson, T. Xiang, and C. Zeng, J. Phys.: Condens. Matter **7**, 8605 (1995).
[14] T. Hikihara, L. Kecke, T. Momoi, and A. Furusaki, Phys. Rev. B **78**, 144404 (2008).
[15] A. V. Chubukov, Phys. Rev. B **44**, 4693(R) (1991).
[16] F. Heidrich-Meisner, I. P. McCulloch, and A. K. Kolezhuk, Phys. Rev. B **80**, 144417 (2009).

[17] J. Sudan, A. Lüscher, and A. M. Läuchli, Phys. Rev. B **80**, 140402(R) (2009).
[18] S. Furukawa, M. Sato, Y. Saiga, and S. Onoda, J. Phys. Soc. Jpn. **77**, 123712 (2008).
[19] T. Vekua, A. Honecker, H.-J. Mikeska, and F. Heidrich-Meisner, Phys. Rev. B **76**, 174420 (2007).
[20] F. Heidrich-Meisner, A. Honecker, and T. Vekua, Phys. Rev. B **74**, 020403(R) (2006).
[21] *Density-Matrix Renormalization*, Lecture Notes in Physics, edited by I. Peschel, X. Wang, M. Kaulke, and K. Hallberg (Springer, Berlin, 1999), Vol. 528.
[22] J. Sirker and A. Klümper, Phys. Rev. B **66**, 245102 (2002).
[23] J. Sirker and A. Klümper, Europhys. Lett. **60**, 262 (2002).
[24] S. Glocke, A. Klümper, and J. Sirker, *Computational Many-Particle Physics*, Lecture Notes in Physics Vol. 739 (Springer, Berlin, 2008).
[25] H. T. Lu, Y. J. Wang, S. Qin, and T. Xiang, Phys. Rev. B **74**, 134425 (2006).
[26] T. Tonegawa and I. Harada, J. Phys. Soc. Jpn. **58**, 2902 (1989).
[27] A. Klümper, Z. Phys. B: Condens. Matter **91**, 507 (1993).
[28] M. Härtel, J. Richter, D. Ihle, and S.-L. Drechsler, Phys. Rev. B **78**, 174412 (2008).
[29] D. V. Dmitriev and V. Y. Krivnov, Phys. Rev. B **73**, 024402 (2006).
[30] D. V. Dmitriev and V. Y. Krivnov, Phys. Rev. B **77**, 024401 (2008).
[31] S. Nishimoto, J. Richter, J. Sirker, S.-L. Drechsler (unpublished).
[32] H.-A. Krug von Nidda, L. E. Svistov, M. V. Eremin, R. M. Eremina, A. Loidl, V. Kataev, A. Validov, A. Prokofiev, and W. Aßmus, Phys. Rev. B **65**, 134445 (2002).
[33] R. D. Somma and A. A. Aligia, Phys. Rev. B **64**, 024410 (2001).
[34] T. Giamarchi, *Quantum Physics in One Dimension* (Clarendon, Oxford, 2004).
[35] L. Kecke, T. Momoi, and A. Furusaki, Phys. Rev. B **76**, 060407(R) (2007).
[36] A. Rusydi, I. Mahns, S. Müller, M. Rübhausen, S. Park, Y. J. Choi, C. L. Zhang, S.-W. Cheong, S. Smadici, P. Abbamonte, M. v. Zimmermann, and G. A. Sawatzky, Appl. Phys. Lett. **92**, 262506 (2008).
[37] N. Motoyama, H. Eisaki, and S. Uchida, Phys. Rev. Lett. **76**, 3212 (1996).
[38] S. Eggert, I. Affleck, and M. Takahashi, Phys. Rev. Lett. **73**, 332 (1994).
[39] J. Sirker, N. Laflorencie, S. Fujimoto, S. Eggert, and I. Affleck, Phys. Rev. Lett. **98**, 137205 (2007).
[40] J. Sirker, N. Laflorencie, S. Fujimoto, S. Eggert, and I. Affleck, J. Stat. Mech.: Theory Exp. 2008, P02015.
[41] J. Sirker and N. Laflorencie, EPL **86**, 57004 (2009).
[42] S. W. Huang, D. J. Huang, J. Okamoto, C. Y. Mou, W. B. Wu, K. W. Yeh, C. L. Chen, M. K. Wu, H. C. Hsu, F. C. Chou, and C. T. Chen, Phys. Rev. Lett. **101**, 077205 (2008).
[43] Long-range chiral order has also recently been found numerically in Refs. 14, 16, and 17 for finite magnetizations.